

OPTIMAL PATHS OF PISTON MOTION OF IRREVERSIBLE DIESEL CYCLE FOR MINIMUM ENTROPY GENERATION

By

Yanlin GE, Lingen CHEN^{}, and Fengrui SUN*

A Diesel cycle heat engine with internal and external irreversibilities of heat transfer and friction, in which the finite rate of combustion is considered and the heat transfer between the working fluid and the environment obeys Newton's heat transfer law [$q \approx \Delta(T)$], is studied in this paper. Optimal piston motion trajectories for minimizing entropy generation per cycle are derived for the fixed total cycle time and fuel consumed per cycle. Optimal control theory is applied to determine the optimal piston motion trajectories for the cases of with piston acceleration constraint on each stroke and the optimal distribution of the total cycle time among the strokes. The optimal piston motion with acceleration constraint for each stroke consists of three segments, including initial maximum acceleration and final maximum deceleration boundary segments, respectively. Numerical examples for optimal configurations are provided, and the results obtained are compared with those obtained when maximizing the work output with Newton's heat transfer law. The results also show that optimizing the piston motion trajectories could reduce engine entropy generation by more than 20%. This is primarily due to the decrease in entropy generation caused by heat transfer loss on the initial portion of the power stroke.

Key words: finite rate of combustion, Newton's heat transfer law, irreversible Diesel cycle heat engine, minimum entropy generation, optimal piston motion trajectories, finite time thermodynamics.

1. Introduction

Since the efficiency bound of a Carnot engine at maximum power output was derived by Curzon and Ahlborn [1], much work [2-14] has been performed in the field of finite-time thermodynamics. The study on the optimal paths of piston motion for internal combustion engines with different optimization objectives and heat transfer laws mainly includes the following two aspects.

1.1. The optimal path with Newton's heat transfer law [$q \approx \Delta(T)$]

Mozurkewich and Berry [15, 16] investigated a four stroke Otto cycle engine with losses of piston friction and heat transfer, in which the heat transfer between the working fluid and the cylinder wall obeys Newton's heat transfer law [$q \approx \Delta(T)$]. The optimal piston trajectory for maximizing the

work output per cycle was derived for the fixed total cycle time and fuel consumed per cycle. The results showed that optimizing the piston motion could improve engine efficiency by nearly 10%. Hoffmann and Berry [17] further considered the effect of the finite combustion rate of the fuel on the performance of engines, and studied the optimal piston motion of a four stroke Diesel cycle engine for maximum work output with losses of piston friction and heat transfer, in which the heat transfer between the working fluid and the cylinder wall also obeys the Newton's heat transfer law. Blaudeck and Hoffman [18] studied the optimal path of a four stroke Diesel cycle with the Newton's heat transfer law by using Monte Carlo simulation. Teh *et al.* [19-21] investigated the optimal piston motions of internal combustion engines for maximum work output [19] and maximum efficiency [20, 21] when the chemical reaction loss and heat leakage are the main losses of internal combustion engine. By excluding the entropy generation due to friction loss, heat transfer loss and pressure drop loss in practical internal combustion engine, Teh *et al.* [22, 23] isolated combustion as the sole source of entropy generation and investigated the optimal piston motion of an adiabatic internal combustion engine for minimum entropy generation [22] as well as the optimal piston motion for minimum entropy generation with fixed compression ratio [23]. Based on the heat engine models established in Refs. [15, 16], Ge *et al.* [24] further considered the entropy generation which was not included in Refs. [22, 23], derived the optimal piston motion trajectories of Otto cycle for minimizing entropy generation due to friction loss, heat transfer loss and pressure drop loss when the heat transfer between the working fluid and the environment obeyed Newton's heat transfer law, and compared the results obtained with those obtained for maximizing the work output with Newton's heat transfer laws [15, 16].

Band *et al* [25, 26] studied optimal configuration of irreversible expansion process for maximum work output obtained from an ideal gas inside a cylinder with a movable piston when the heat transfer between the gas and the bath obeyed Newton's heat transfer law, and discussed the optimal configurations of the expansion subjected to eight different constraints, including constrained rate of change of volume, unconstrained final volume, constrained final energy and final volume, constrained final energy and unconstrained final volume, consideration of piston friction, consideration of piston mass, consideration of gas mass and unconstrained total process time, respectively. Salamon *et al* [27] and Aizenbud and Band [28] used the results obtained in Refs. [25, 26] to further investigate the optimal configurations of the expansion process for maximizing power output [27] and the optimal configurations for maximizing work output with fixed power output [28] with Newton's heat transfer law. Aizenbud *et al* [29] and Band *et al* [30] further applied the results obtained in Refs. [25, 26] to optimize the configurations of internal [29] and external [30] combustion engines with Newton's heat transfer law, respectively.

1.2. The effect of heat transfer law on the optimal path of cycle

In general, heat transfer is not necessarily Newtonian and also obeys other laws; heat transfer law has the significant influence on the optimal configuration of heat engine cycles. Burzler and Hoffman [31, 32] considered the effects of convective-radiative heat transfer law [$q \approx \Delta(T) + \Delta(T^4)$] and non-ideal working fluid, and derived the optimal piston motion for maximizing power output during the compression and power strokes of a four stroke Diesel engine. Xia *et al* [33] studied the optimal piston trajectory of the Otto cycle engine for maximizing work output with fixed total cycle

time, the fixed fuel consumed per cycle and linear phenomenological heat transfer law [$q \approx \Delta(T^{-1})$] in the heat transfer process between working fluid and the environment, and the results showed that optimizing the piston motion could improve work output and efficiency of the engine by more than 9% .

Based on the heat engine models established in Refs. [15, 16, 33], Ge *et al* [24, 34] derived the optimal piston motion trajectories of Otto cycle for minimizing entropy generation due to friction loss, heat transfer loss and pressure drop loss when the heat transfer between the working fluid and the environment obeys linear phenomenological [24] and radiative [34] heat transfer laws, and compared the results obtained with those obtained for maximizing the work output with Newton's [15, 16] and linear phenomenological [33] heat transfer laws.

On the basis of Ref. [26], Chen *et al* [35] determined the optimal configurations of expansion process of a heated working fluid in the piston cylinder with the linear phenomenological heat transfer law. Song *et al* [36] and Chen *et al* [37] used the results obtained in Ref. [35] to optimize the configuration of external [36] and internal [37] combustion engines with linear phenomenological heat transfer law. Song *et al* [38], Ma *et al* [39] and Chen *et al* [40] determined the optimal configurations of expansion process of a heated working fluid in the piston cylinder with the generalized radiative [$q \propto \Delta(T^n)$] [38], Dulong-Petit [$q \propto \Delta(T)^{5/4}$] [39] and convective-radiative [40] heat transfer laws, obtained the first-order approximate analytical solutions about the Euler-Lagrange arcs by means of Taylor series expansion. Ma *et al* [41, 42] repeated the investigation on the optimal configurations of expansion process with the generalized radiative heat transfer law by means of elimination method. Ma *et al* [41, 43] used the results obtained in Refs. [41, 42] to optimize the configuration of external combustion engine with radiative [$q \approx \Delta(T^4)$] [41, 43], generalized radiative [43] and convective-radiative [41] heat transfer laws, respectively. Chen *et al* [44] considered the effects of piston motion on the heat conductance, established a model closer to practical expansion process of heated working fluid with the generalized radiative heat transfer law and time-dependent heat conductance, and determined optimal configuration of expansion process for maximum work output.

Based on Refs. [17, 24], this work studies the optimal piston trajectory of the Diesel cycle engine for minimizing entropy generation per cycle with the finite rate of combustion, the fixed total cycle time, the fixed fuel consumed per cycle and Newton's heat transfer law in the heat transfer process between working fluid and environment, and the results obtained are compared with those obtained for maximizing the work output with the Newton's heat transfer law [17].

2. Diesel cycle engine model

In order to analyze practical Diesel cycle, some assumptions are made: (1) the fixed fuel consumed per cycle is equivalent to the given initial working fluid temperature on the power stroke; (2) the working fluid in the cylinder consists of an ideal gas which is in internal equilibrium all the time; and (3) the major losses in real internal combustion engine and the piston motion of the conventional engine are simplified and described qualitatively and quantitatively below according to Refs.[15-18, 24, 33, 45, 46].

2.1. Finite combustion rate [17]

In the modern Diesel cycle engine, fuel is injected into the cylinder at the end of the compression stroke and evaporates in the hot compressed air. After a short delay, part of the injected fuel is ignited and burned rapidly. The remaining fuel burns relative slowly as it evaporates and diffuses into oxygen-rich regions where combustion can be sustained. In moderately and heavily loaded engines, the combustion process will continue until the end of the power stroke.

The finite combustion rate is one of the main features of a Diesel engine and can be approximated by the following time-dependent function which describes the extent of the reaction [17]

$$G(t) = F + (1 - F)[1 - \exp(-t / t_b)] \quad (1)$$

where F is the fraction of the fuel charge consumed in the initial instantaneous burn, and t_b is the burn time during which most of the combustion occurs. For the corresponding heating function $h(t)$, one has

$$h(t) = NQ_c \dot{G}(t) \quad (2)$$

where Q_c is the heat of combustion per molar fuel-air mixture charge. Q_c is assumed to be temperature independent.

The mole number N and heat capacity C are assumed to be influenced by the extent of the combustion reaction within the piston chamber. This dependence can be expressed as [17]

$$N = N(t) = N_i + (N_f - N_i)G(t) \quad (3)$$

$$C = C(t) = C_i + (C_f - C_i)G(t) \quad (4)$$

The subscripts i and f refer to conditions at $G = 0$ and $G = 1$, respectively. Furthermore, the heat capacities of the reactants and products are temperature independent.

2.2. Loss terms [15-18, 24, 33, 45]

For the Diesel cycle, the major losses are as follows: (1) friction, (2) pressure drop, (3) heat leakage, (4) fuel injection, (5) incomplete combustion, and (6) exhaust blowdown. The non-negligible losses from this list are cast into simplified functional forms and incorporated into this model. This approach reproduces the Diesel engine's salient features in a flexible, easily decipherable model.

2.2.1. Friction loss

Friction force is assumed to be proportional to the piston velocity v [15-18, 24, 33], the frictional work W_f in a stroke taking time t is expressed as

$$W_f = \int_0^t \mu v^2 dt \quad (5)$$

Due to greater pressure on the piston, the value of friction coefficient is usually about twice as large on the power stroke as on the other strokes. If the friction coefficient on the nonpower stroke is μ , the friction coefficient on the power stroke will be 2μ [15-18, 24, 33].

2.2.2. Pressure drop

There is an additional friction-like loss term on the intake stroke. This is due to the pressure differential that develops, due to viscosity, as the gas flows through the inlet valve. The pressure differential is proportional to velocity, so it may be included in the friction term for the intake stroke, and then the friction coefficient on the intake stroke is assumed to be 3μ [15-18, 24, 33].

2.2.3. Heat leakage

Loss due to heat transfer from the working fluid to cylinder walls typically cost about 12% of the total power [45]. The same as Refs. [15-18, 24], the heat transfer between the working fluid and the environment obeys Newton's heat transfer law. The heat transfer expression used here assumes that the rate is linear in the inside surface area of the cylinder and in the difference between the temperature of working fluid T and that of the cylinder wall T_w . T_w is assumed to be a constant. For heat transfer coefficient k and cylinder diameter b , the rate of heat leakage at position X (see fig. 1) is

$$\dot{Q} = k\pi b(b/2 + X)(T - T_w) \quad (6)$$

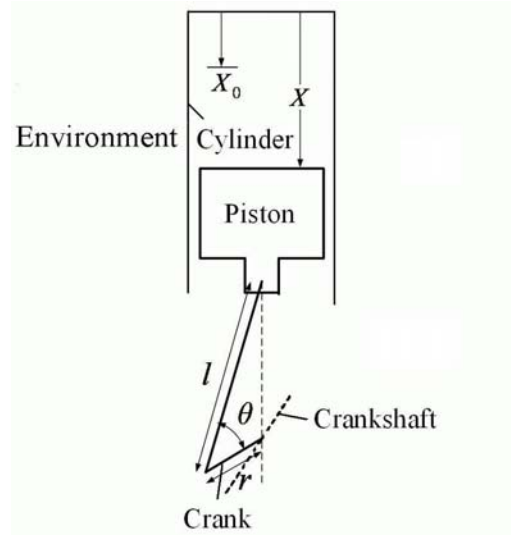


Figure 1. Conventional piston linkage.

The effect of heat transfer is only important on the power stroke. Since the average value of $(T - T_w)$ is much smaller on the nonpower stroke, the rate is negligible on them.

2.2.4. Incomplete combustion

If the exhaust valve opens before the burning fuel-air mixture reaches chemical equilibrium, there can be minor efficiency losses even in well-adjusted engines operating at normal loads. These losses have been included in the model by representing the combustion reaction as the exponential function give explicitly in eq. (1) [17].

2.2.5. Other losses

Besides, there are effects of the time loss due to beginning the expansion stroke while combustion is still taking place and the exhaust blowdown due to opening the exhaust valve before completion of the expansion stroke. They are so small compared with the heat leakage and friction losses that they are all negligible [24].

2.3. Piston motion of a conventional engine [46]

To determine improvements resulting from the optimized piston motion, work output and engine efficiencies are calculated for conventional piston trajectories. Piston motion within a conventional Diesel engine can be described by

$$v = \dot{X} = \frac{2\pi\Delta X \sin \theta}{\tau} \left\{ 1 + \frac{r \cos \theta}{l} \left[1 - \left(\frac{r}{l} \right)^2 \sin^2 \theta \right] \right\}^{-1/2} \quad (8)$$

As shown in fig. 1, X denotes piston position, $\Delta X = 2r$, and $\theta = 4\pi t/\tau$. $X = X_0$ when $t = 0$. The four-stroke cycle period is τ . Pure sinusoidal piston motion occurs when $r/l = 0$. Typical r/l is between 0.16 and 0.40. Varying the value of r/l has little effect on the results.

3. Optimization procedure

The optimization problem is minimizing the entropy generation per cycle for fixed fuel consumption and total cycle time. Thus, the only difference between the optimized engine and the conventional one is in the piston motion. The optimization procedure consists of two parts. The first is to determine the optimal trajectory on each stroke. The second is to optimize the distribution of the total cycle time among the strokes. A real engine includes power and nonpower strokes. Compared with the power stroke, the heat leakage is negligible on the nonpower strokes which include intake, compression and exhaust strokes. Therefore, the optimization of these strokes is relatively simple, and the three strokes can be treated together to simplify the optimization problem. For the three nonpower strokes, at first, the piston path on each stroke is determined with the objective of minimum entropy generation, respectively, and then the time allocation among three non-power strokes for a fixed total time t_{np} is determined with the objective of minimum total entropy generation $\Delta S_{t_{np}}$. While for the power stroke, the piston path is determined with the objective of minimum entropy generation ΔS_{t_p} when heat transfer loss is considered. For the total cycle, the distribution of the total cycle time τ between the total time t_{np} of nonpower strokes and the power stroke time t_p is determined with the objective of minimum entropy generation ΔS per cycle.

3.1. Optimization for nonpower strokes

The optimal process of nonpower strokes is the same as Ref. [24]. After optimization, the total entropy generation on nonpower strokes is

$$\Delta S_{t_{np}} = \mu a_m^2 [2t_1^3(1+2y_1)(1-y_1)^2 + 3t_2^3(1+2y_2)(1-y_2)^2] / (12T_0) \quad (9)$$

For a given value of nonpower stroke time t_{np} , the optimal allocation of the nonpower stroke time is determined by following two equations

$$t_{np} = 2t_1 + t_2 \quad (10)$$

$$t_1^2(1-y_1)^2 = 3t_2^2(1-y_2)^2 \quad (11)$$

where $y_1 = (1-4\Delta X / a_m t_1^2)^{1/2}$, $y_2 = (1-4\Delta X / a_m t_2^2)^{1/2}$ and a_m is the value of constrained acceleration.

For the case without constraint on acceleration, i.e. $a_m \rightarrow \infty$, eq. (11) becomes

$$t_2 = \sqrt{3}t_1 \quad (12)$$

And the total entropy generation, from eq. (9), is

$$\Delta S_{t_{np}} = \mu(2 + \sqrt{3})^2 (\Delta X)^2 / (t_{np} T_0) \quad (13)$$

3.2. Optimization for power stroke

Different from the optimization of the nonpower strokes, in which only the friction loss is considered, the optimization of the power stroke will consider the effects of heat transfer on the optimal piston trajectory. So, the entropy generation in power stroke is due to friction loss and heat transfer loss, and which can be expressed as $\Delta S_{f,p}$ and $\Delta S_{q,p}$, respectively.

$$\Delta S_{f,p} = \frac{\int_0^{t_p} 2\mu v^2 dt}{T_0} \quad (14)$$

$$\Delta S_{q,p} = \frac{\int_0^{t_p} k\pi b(b/2 + X)(T - T_w) dt}{T_0} \quad (15)$$

3.2.1. Power stroke with unconstrained acceleration

In order to obtain the minimum entropy generation during the power stroke, the corresponding optimization problem becomes

$$\min \Delta S_{t_p} = \Delta S_{f,p} + \Delta S_{q,p} = \frac{\int_0^{t_p} [2\mu v^2 + k\pi b(b/2 + X)(T - T_w)] dt}{T_0} \quad (16)$$

In terms of the first law of thermodynamics, one has

$$\dot{T} = -\frac{1}{NC} \left[\frac{NRTv}{X} + k\pi b \left(\frac{b}{2} + X \right) (T - T_w) - h(t) \right] \quad (17)$$

where R is the gas constant. The rate of heat produced during the combustion is described by the heating function

$$h(t) = \frac{NQ_c(1-F)}{t_b} \exp\left(-\frac{t}{t_b}\right) \quad (18)$$

Furthermore, there is

$$\dot{X} = v \quad (19)$$

The Hamiltonian for this problem is

$$H = \frac{2\mu v^2 + k\pi b(b/2 + X)(T - T_w)}{T_0} - \frac{\lambda_1}{NC} \left[\frac{NRTv}{X} + k\pi b \left(\frac{b}{2} + X \right) (T - T_w) - h(t) \right] + \lambda_2 v \quad (20)$$

The canonical equations are

$$\dot{\lambda}_1 = -\frac{\partial H}{\partial T} = k\pi b\left(\frac{b}{2} + X\right)\left(\frac{\lambda_1}{NC} - \frac{1}{T_0}\right) + \frac{\lambda_1 Rv}{CX} \quad (21)$$

$$\dot{\lambda}_2 = -\frac{\partial H}{\partial X} = k\pi b(T - T_w)\left(\frac{\lambda_1}{NC} - \frac{1}{T_0}\right) - \frac{\lambda_1 RTv}{CX^2} \quad (22)$$

The extremum condition is $\partial H / \partial a = 0$, one has

$$v = \frac{T_0(\lambda_1 RT - \lambda_2 CX)}{4\mu CX} \quad (23)$$

In solving these equations, there are four boundary conditions to be satisfied. They are

$$T(0) = T_{0p}, \quad X(0) = X_0, \quad X(t_p) = X_f, \quad \lambda_1(t_p) = 0 \quad (24)$$

where T_{0p} is the initial temperature of working fluid on the power stroke. Eqs. (17), (19), (21) and (22) determine the optimal solution of this problem, which could be solved for the minimum value of ΔS_{ip} as a function of time and the optimal path of piston motion, i.e. optimal relationship between piston velocity v and time t when the power stroke time t_p is given.

Furthermore, the initial position of the piston must be constrained, and the piston position during the whole power stroke should satisfy the following equation

$$X \geq X_0 \quad (25)$$

Without the above constraint the piston will move above the top dead center. After constrained the piston position, the optimal path of the piston with unconstrained acceleration on the power stroke is a two branch path. For $0 \leq t \leq t_d$, the velocity of piston is

$$v(t) = 0 \quad (26)$$

where t_d is the motion delay time. During the motion delay time t_d , the piston position will not satisfy the eq. (25), and the piston must keep still. While for $t_d \leq t \leq t_p$, the piston position will satisfy the eq. (25), and the velocity of piston will be eq.(23).

3.2.2. Power stroke with constrained acceleration

For the case with constrained acceleration, the piston velocity is required to be zero at both start and end points and the acceleration is constrained to lie within finite limits. The optimization objective is still to minimize the function given by eq. (16), the differential constraints on the state variables T and X remain as given in eqs. (17) and (19), respectively. Besides, the dependence of the state variable v on the control variable a and the inequality constraints on variable a are given by

$$\dot{v} = a \quad (27)$$

$$-a_m \leq a \leq a_m \quad (28)$$

The Hamiltonian for this problem is

$$H = \frac{2\mu v^2 + k\pi b(b/2 + X)(T - T_w)}{T_0} - \frac{\lambda_1}{NC} \left[\frac{NRTv}{X} + k\pi b(b/2 + X)(T - T_w) - h(t) \right] + \lambda_2 v + \lambda_3 a \quad (29)$$

The canonical equations conjugate to eqs. (17), (19) and (27) are eqs. (21), (22) and

$$\dot{\lambda}_3 = -\frac{\partial H}{\partial v} = -\frac{4\mu v}{T_0} + \frac{\lambda_1 RT}{CX} - \lambda_2 \quad (30)$$

The extremum condition is $\partial H / \partial a = 0$, one has

$$\lambda_3 = 0 \quad (31)$$

If eq. (31) holds for more than isolated points between $-a_m$ and a_m , one also has

$$\dot{\lambda}_3 = 0 \quad (32)$$

Eliminating λ_3 by using eqs. (30) and (32), the expression of the velocity is the same as eq. (23). On this basis one can conclude that the optimal trajectory with acceleration constraint on the power stroke has two cases. The first case is that when the piston motion exists motion delay time t_d , the optimal trajectory is a three-branch path: (1) From the initial time $t = 0$ to the motion delay time $t = t_d$, the piston keeps still, and the piston position is the initial position. (2) From the motion delay time $t = t_d$ to the switch time $t = t'$, the piston trajectory satisfies the system of eqs. (17), (19), (21) and (22). (3) From the switch time $t = t'$ to the power stroke time $t = t_p$, the piston trajectory is the maximum deceleration segment. The second case is that when the piston motion does not exist motion delay time t_d , i.e. the piston position is $X \geq X_0$ during the whole power stroke time, the optimal trajectory is also a three-branch path, i.e. two boundary segments (maximum acceleration and maximum deceleration) connected by a segment which satisfies the system of eqs. (17), (19), (21) and (22). For these equations, only numerical results could be obtained.

4. Numerical examples and discussions

4.1. Determination of the related constants and parameters

Table 1. Constants and parameters used in the calculations [14]

Mechanical parameters	
initial position	$X_0 = 0.5cm$
final position	$X_f = 8cm$
cylinder bore	$b = 7.98cm$
cycle time	$\tau = 33.3ms$ corresponding to 3600 rpm
Thermodynamic parameters	
number of moles of gas	compression stroke $N_i = 0.0144$, power stroke $N_f = 0.0157$
initial temperature	compression stroke $T_{0c} = 329K$, power stroke $T_{0p} = 2360K$
constant volume heat capacity	compression stroke $C_i = 2.5R$, power stroke $C_f = 3.35R$
cylinder wall temperature	$T_w = 600K$
Loss term coefficients	
friction coefficient	$\mu = 12.9kg / s$
heat transfer coefficient	$k = 1305W \cdot K^{-1} \cdot m^{-2}$
Heat function parameters	
explosion fraction	$F = 0.5$
burn time	$t_b = 2.5ms$
heat of combustion	$Q_c = 5.75 \times 10^4 J / mol$ per molar fuel-air mixture charge
Gas constant	$R = 8.314J \cdot mol^{-1} \cdot K^{-1}$

In order to calculate the entropy generation, the environment temperature $T_0 = 300K$ is set.

Other constants and parameters are listed in tab. 1 according to Ref. [17].

In the following calculations, v_{\max} is the maximum velocity of the piston on the power stroke and T_f is temperature of working fluid at the end of power stroke.

4.2. Numerical examples for the case with constrained acceleration

The optimal trajectory with constrained acceleration on the power stroke is a three-branch path. The system of differential equations for the case with constrained acceleration is solved backwards, i.e. taking the final position of the piston as the initiate point of calculation. For the piston motion maybe exists motion delay time, the detail calculation method has two cases.

(1) There is exist the motion delay time of piston motion

When the time t_p spent on the power stroke is fixed, the first is to calculate the maximum deceleration segment. The values of the final temperature T_f and the time spent on the maximum deceleration segment t_{p3} are guessed, then solving eqs. (17), (19) and (25) for the initial various parameters on this segment. The second is to calculate the interior segment. Using the calculation results of the former step as the initial values of this step, one can solve the differential equations (17), (19), (21) and (22) backwards with the iterative method. $X - X_0 < 0$ is used as the terminate condition of the calculating process. The time spent on this segment t_{p2} can be obtained, and the motion delay time can be written as $t_d = t_p - t_{p3} - t_{p2}$. The third is to calculate the first segment During the motion delay time, the piston position is initial position and velocity keep still, i.e. $X = X_0$ and $v = 0$. The initial temperature T_{0p} can be solved by eq. (17). The resultant value of T_{0p} is compared with the desired one. The guessed initial value of T_f and the time spent on the maximum deceleration segment t_{p3} are then modified to minimize the square of the deviation between the resultant and desired values, and the entropy generation on the power stroke ΔS_{t_p} is solved. The fourth is to calculate the entropy generation and the time distribution of nonpower strokes. Using the calculation result of the time spent on the power stroke t_p , one can solve eqs. $t_{np} = \tau - t_p = 2t_1 + t_2$, (9) and (11) for the entropy generation $\Delta S_{t_{np}}$ and time distribution of nonpower strokes, and then the total entropy generation of the cycle ΔS can be obtained. The fifth is to modify the value of the time spent on the power stroke t_p , and to repeat the former four steps until all of the values of the time spent on the power stroke are calculated. The sixth is to compare the entropy generation per cycle ΔS with different values of time spent on the power stroke and to select the minimum ΔS .

(2) There is not exist the motion delay time of piston motion

When the time t_p spent on the power stroke is fixed, the first is to calculate the maximum deceleration segment. The values of the final temperature T_f and the time spent on the maximum deceleration segment t_{p3} are guessed, then solving eqs. (17), (19) and (25) for the initial various parameters on this segment. The second is to calculate the interior segment. Using the calculation results of the former step as the initial values of this step, one can solve the differential equations (17), (19), (21) and (22) backwards with the iterative method. The piston velocity on the initial position of the interior segment is related to the piston position, which could be a switching point from the interior segment to the maximum acceleration segment. The initial parameters and the time spent on this segment t_{p2} can be obtained. The third is to calculate the maximum acceleration segment. Using the calculation results of the former step as the initial values of this step, one can solve eqs. (17), (19) and (25) backwards for the initial temperature T_{0p} and the time spent on the maximum acceleration

segment t_{p1} . The resultant values of T_{0p} and the total time spent on the three segments $t_{p1} + t_{p2} + t_{p3}$ are compared with the desired ones. The guessed initial values of T_f and the time spent on the maximum deceleration segment t_{p3} are then modified to minimize the square of the deviation between the resultants and desired values, and the entropy generation on the power stroke ΔS_{t_p} is solved. The fourth is to calculate the entropy generation and the time distribution of nonpower strokes. Using the calculation result of the time spent on the power stroke t_p , one can solve eqs. $t_{np} = \tau - t_p = 2t_1 + t_2$, (9) and (11) for the entropy generation $\Delta S_{t_{np}}$ and time distribution of nonpower strokes, and then the total entropy generation of the cycle ΔS can be obtained. The fifth is to modify the value of the time spent on the power stroke t_p , and to repeat the former four steps until all of the values of the time spent on the power stroke are calculated. The sixth is to compare the entropy generation per cycle ΔS with different values of time spent on the power stroke and to select the minimum ΔS .

Table 2 . Parameters for different cases

Case	Variation from Table 1
1	none
2	$t_b = 0.1ms$
3	$t_b = 1.0ms$
4	$t_b = 5.0ms$
5	$\tau = 66.66ms$,corresponding to 1800rpm
6	$k = 2610W \cdot K / m^2$
7	$\mu = 25.8kg / s$

Tab. 2 lists some parameters (other parameters unchanged) varied from tab. 1. Tab. 3 lists the calculation results for the corresponding cases, where the modified sinusoidal motion ($r/l = 0.25$) is chosen as the conventional motion. From tab. 3, one can see that the influences of different choices of burn time, friction coefficient, heat leakage coefficient and cycle time on the optimal configurations of piston movement. For different cases, the results in tab. 3 show that the peak velocity v_{max} is much larger than that of with the conventional motion, while the time spent on power stroke t_p with the optimal piston motion is smaller than that of with conventional motion, respectively. After optimization, the decrease of time spent on the power stroke t_p has two influences. On the one hand, with the decrease of t_p , the time spent on the nonpower strokes t_{np} will increase and the mean piston velocity during the nonpower strokes will decrease, so the entropy generation due to the friction loss on the nonpower strokes will decrease which can be seen from the change of $\Delta S_{t_{np}}$ in tab. 3. On the other hand, with the decrease of t_p , the heat leakage loss will decrease for the decrease in the time spent on the contact between the high-temperature working fluid and the environment outside the cylinder, so the entropy generation due to heat leakage loss on the power stroke will decrease which can be seen from the change of $\Delta S_{q_{t_p}}$ in tab. 3. The entropy generation due to friction loss on the power stroke will increase with the increase of the peak velocity, this can be seen from the change of $\Delta S_{f_{t_p}}$. The amount of increase in the entropy generation due to friction losses is always smaller than the amount of the decrease in the entropy generation due to heat leakage loss on the power stroke, so the total entropy generation on the power stroke is decreased, which can be seen from the change of

ΔS_{t_p} in tab. 3. Both the entropy generations on the nonpower strokes and power stroke are decreased, so the entropy generations per cycle ΔS with the optimal piston motion are smaller than those with the conventional piston motion.

Table 3. Numerical results for different cases with constrained acceleration $a_m = 3 \times 10^4 m \cdot s^{-2}$

Case		v_{\max}	t_p	$\Delta S_{t_{np}}$	$\Delta S_{f_{sp}}$	$\Delta S_{q_{sp}}$	ΔS_{t_p}	ΔS	T_f
		m/s	ms	$J \cdot K^{-1}$	$J \cdot K^{-1}$	$J \cdot K^{-1}$	$J \cdot K^{-1}$	$J \cdot K^{-1}$	K
1	conv.	13.3	8.33	0.1585	0.0634	0.6576	0.7210	0.8795	1242
	opt.	39.6	3.20	0.1119	0.1962	0.2724	0.4686	0.5805	1371
2	conv.	13.3	8.33	0.1585	0.0634	0.6637	0.7271	0.8856	1165
	opt.	40.5	3.20	0.1119	0.1971	0.3598	0.5569	0.6688	1619
3	conv.	13.3	8.33	0.1585	0.0634	0.6472	0.7106	0.8691	1182
	opt.	39.9	3.20	0.1119	0.1964	0.3268	0.5232	0.6351	1501
4	conv.	13.3	8.33	0.1585	0.0634	0.6329	0.6963	0.8548	1223
	opt.	40.2	3.20	0.1119	0.1972	0.2287	0.4259	0.5378	1200
5	conv.	6.7	16.65	0.0792	0.0317	0.9299	0.9616	1.0408	949
	opt.	39.6	3.20	0.0531	0.1962	0.2724	0.4686	0.5217	1371
6	conv.	13.3	8.33	0.1585	0.0643	0.9411	1.0045	1.1630	1000
	opt.	40.5	3.20	0.1119	0.1976	0.4989	0.6965	0.8084	1242
7	conv.	13.3	8.33	0.3170	0.1268	0.6576	0.7844	1.1014	1247
	opt.	28.2	3.60	0.2269	0.3196	0.3089	0.6285	0.8554	1371

4.3. Comparison between the optimal and conventional piston motions

Table 4. Result comparison between optimal trajectories with constrained acceleration and conventional engines

Case	Decrease in	Decrease in	Decrease in	Decrease in	Decrease in
	$\Delta S_{t_{np}}$	$\Delta S_{f_{sp}}$	$\Delta S_{q_{sp}}$	ΔS_{t_p}	ΔS
1	0.0466	-0.1328	0.3852	0.2524	0.2990
2	0.0466	-0.1337	0.3039	0.1702	0.2168
3	0.0466	-0.1330	0.3204	0.1874	0.2340
4	0.0466	-0.1338	0.4042	0.2704	0.3170
5	0.0261	-0.1645	0.6575	0.4930	0.5191
6	0.0466	-0.1333	0.4422	0.3090	0.3556
7	0.0901	-0.1928	0.3487	0.1559	0.2460

Tab. 4 lists the comparison results between the optimal trajectory and the conventional motion for different cases with constrained acceleration. From the amounts of the decreases of $\Delta S_{t_{np}}$ and $\Delta S_{f_{sp}}$ listed in tab. 4, one can see that the amount of the decrease of the entropy generation $\Delta S_{t_{np}}$ due to the friction loss on the nonpower strokes is smaller than that of the increase of the entropy generation $\Delta S_{f_{sp}}$ due to the friction loss on the power stroke after optimizing the piston motion, the entropy generation of the cycle due to friction loss increases after the optimization. Although the entropy generation of the cycle due to friction loss increases, the total entropy generation of the cycle

decreases after the optimization. From the amount of the decrease of $\Delta S_{q,p}$ listed in tab. 4, one can see that, for the whole cycle, the amount of the decrease of the entropy generation due to the heat leakage loss is much larger than that of the increase of the entropy generation due to the friction loss, the total optimization process is realized by decreasing the entropy generation due to heat leakage loss on the initial portion of the power stroke. Comparing the optimization results of cases 1-4, one can see that the optimization effect is better when the burn time is longer. Comparing the optimization results of cases 1 and 5, one can see that the optimization effect is better when the cycle period is longer. Furthermore, figs. 2-4 show the comparison of the optimal and conventional piston motions on the power stroke for case 1.

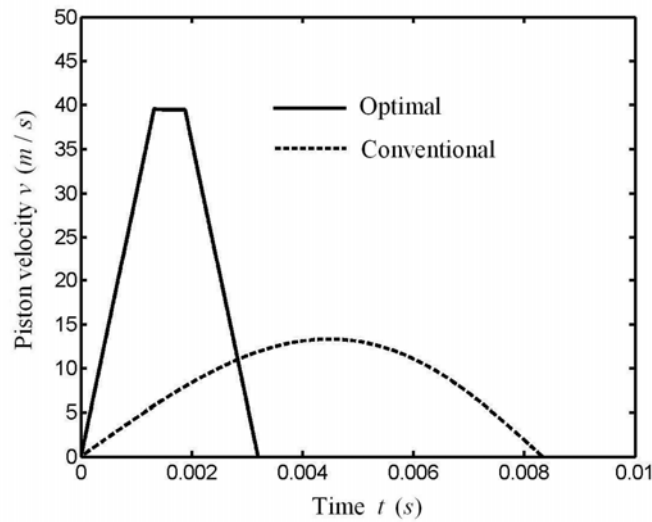


Figure 2. Comparison of piston velocity of optimal and conventional motions on the power stroke for case 1

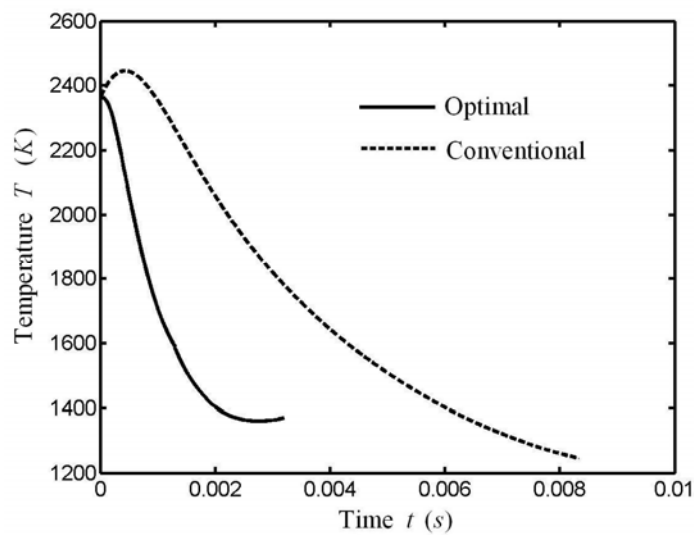


Figure 3. Comparison of working fluid temperature of optimal and conventional motions on the power stroke for case 1

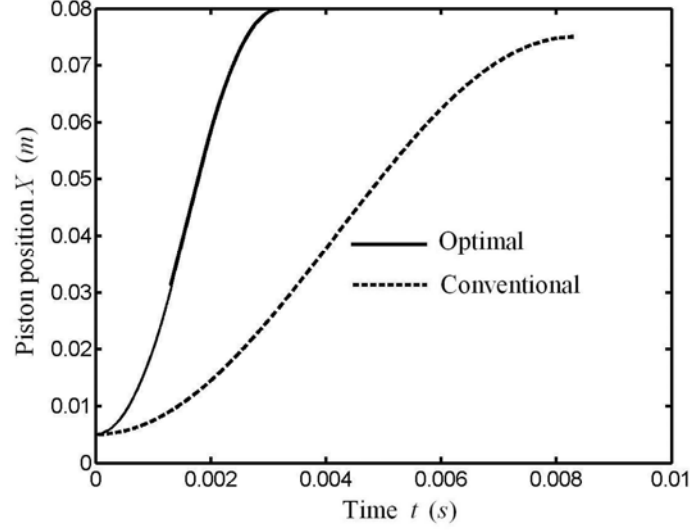


Figure 4. Comparison of piston position of optimal and conventional motions on the power stroke for case 1

4.4. Comparison between the optimal piston motions with different optimization objectives.

Figs. 5-7 show the optimal piston trajectories on the power stroke with two different optimization objectives, which include the optimal trajectory with maximum work output (power operating regime) [15] and minimum entropy generation (economical operating regime) (this paper). Tab. 5 lists the corresponding results of numerical calculations. In Tab. 5, $\varepsilon = W_\tau / W_R$ is the effectiveness, i.e. the second-law efficiency [47]. When heat transfer is considered, the reversible process which corresponds to the practical expansion process of Diesel cycle after optimizing the piston motion is not a reversible adiabatic expansion process, but a reversible polytropic process, so the reversible work output per cycle which corresponds to the practical cycle after optimization should be

$$W_R = N_p R(T_{0p} - T_f) / (n-1) + N_c C_{vc} T_{0c} [1 - (X_f / X_0)^{R/C_c}] \quad (31)$$

where n is the polytropic exponent. The first part of eq. (31) $N_p R(T_{0p} - T_f) / (n-1)$ is used to calculate the reversible expansion work of reversible polytropic process. When optimizing the piston motion, the heat leakage along the nonpower strokes is negligible, so the reversible process which corresponds to the practical compression process after optimization is still a reversible adiabatic compression process. The second part of eq. (31) $N_c C_{vc} T_{0c} [1 - (X_f / X_0)^{R/C_c}]$ is used to calculate the reversible compression work of reversible adiabatic compression process. According to Ref. [48], the polytropic exponent changes during the expansion process of Diesel engine, and usually the mean polytropic exponent of the expansion is $n = 1.22 \sim 1.28$. In this paper, $n = 1.25$ is used.

W_p is the work output on the power stroke, $W_{f,np}$ is the work lost due to the friction loss on the nonpower strokes, and W_{com} is the required compression work input along the nonpower strokes, so the net work output per cycle is $W_\tau = W_p - W_{f,np} - W_{com}$.

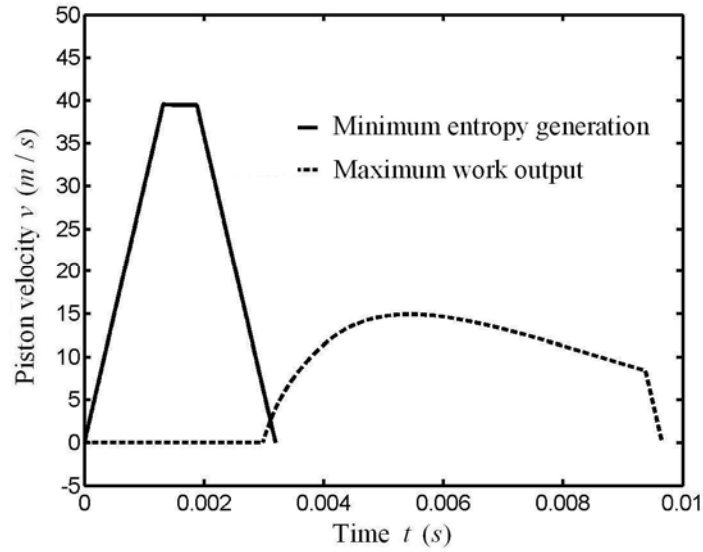


Figure 5. Comparison of piston velocity on the power stroke for two optimization objectives

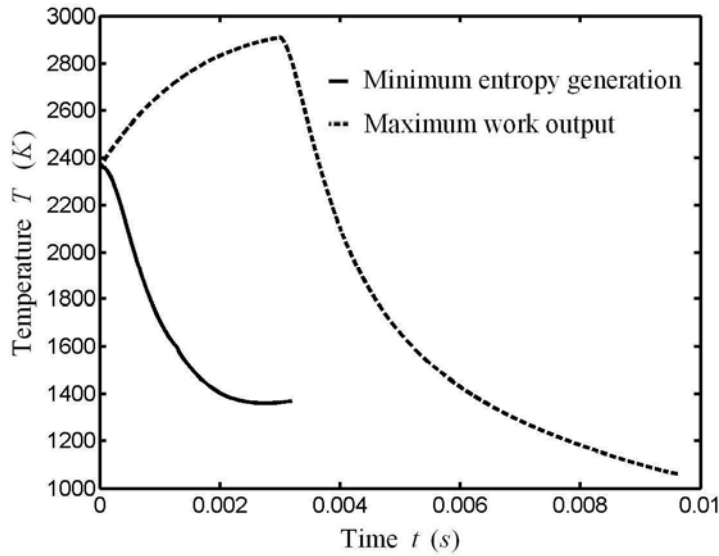


Figure 6. Comparison of working fluid temperature on the power stroke for two optimization objectives

Comparing the results of numerical calculations with two optimization objectives listed in tab. 5, one can see that the entropy generation and work output with the minimum entropy generation objective decrease by 47% and 45%, respectively, while the efficiency increases by 25%.

From figs. 5-7, as is also shown by paper [49], one can see that optimization results are essentially different for two optimization objectives. The similarities for the optimal piston motions with different optimization objectives are as follows: They both consist of three segments, including two boundary segments and a middle movement segment; both the last segments are maximum

deceleration segment; both the middle movement segments and corresponding optimal solutions with unconstrained acceleration satisfy the same differential equations. While the differences for the optimal piston motions with different optimization objectives are: The first segment with the minimum entropy generation objective is a maximum acceleration segment, while that with maximum work output objective is a stock-still segment. The reason for the differences is: With the maximum work output objective, the piston motion has a delay time on the power stroke, during the delay time the piston is stock-still and the temperature of the working fluid increases rapidly with the fuel combustion (which can be seen from the variation of the temperature in fig. 6), so the increase of the temperature of the working fluid at the beginning of the power stroke increases the piston expansion work output (which can be seen from the variation of W_p in tab. 5). In addition, from the results listed in tab. 5, one can see that the optimal times t_p spent on the power stroke with different optimization objectives are different, i.e. the optimal distributions of the total cycle time τ among the strokes are distinct. Both the two above kinds of differences show that optimization objective has important effects on the optimal piston trajectory.

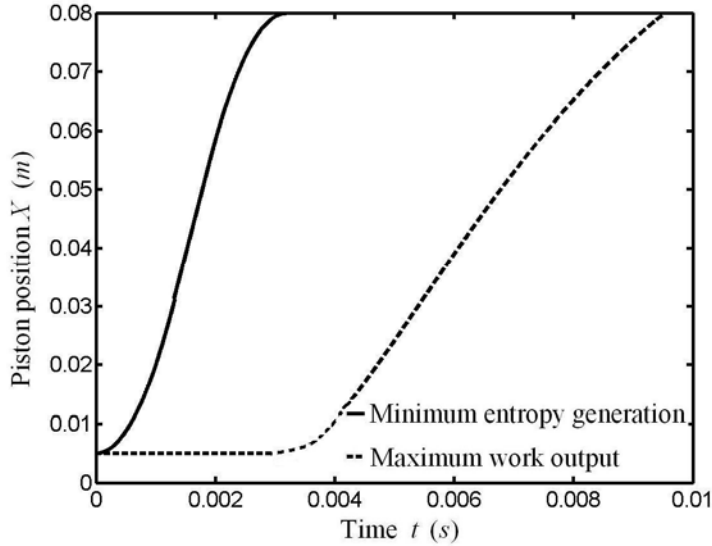


Figure 7. Comparison of piston position on the power stroke for two optimization objectives

Table 5. Numerical results for the optimal piston trajectories of power stroke with two optimization objectives

Optimal objective	v_{\max}	t_p	ΔS_{t_p}	W_R	W_p	W_τ	$W_{f,x}(J)$		Q	T_f	ε
	m/s	ms	$J \cdot K^{-1}$	J	J	J	$W_{f,\Delta p}$	$W_{f,\Delta p}$	J	K	
Minimum entropy generation	39.56	3.2	0.4686	388.6	507.3	277.4	33.6	58.9	81.7	1371	0.714
Maximum work output	14.97	9.66	0.8838	837.1	740.2	501.1	42.8	24.5	241.1	1061	0.598

5. Conclusion

On the basis of Refs. [17, 24], this paper studies a Diesel cycle engine with internal and

external irreversibilities of friction and heat leakage, in which the finite rate of combustion is considered and the heat transfer between the working fluid and the cylinder wall obeys the Newton's heat transfer law. The optimal piston trajectories for minimum the entropy generation per cycle are derived for the fixed total cycle time and fuel consumed per cycle. Optimal control theory is applied to determine the optimal piston trajectories for the cases of unconstrained and constrained piston accelerations on each stroke and the optimal distribution of the total cycle time among the strokes. The main conclusions include: (1) The optimal piston motions with minimum entropy generation and maximum work output optimization objectives consist of three segments, including two boundary segments and a middle movement segment, the first segment of the optimal piston motion with the minimum entropy generation objective is a maximum acceleration segment, while that with maximum work output objective is a stoke-still segment. There are in fact several ways of achieving those pathways of which one points out just two: one mechanical solution is using a contoured plate to guide the piston on the desired path as shown in fig. 8 (i.e. an eccentric shaft of properly designed shape turns the optimal motion of the piston into a constant angular rotation) [see page 42 of Ref. [50] in detail], and another completely different way to transform the optimized paths is the use of an electrical coupling, see page 42 of Ref. [50] in detail. (2) After minimum entropy generation optimization, the amount of the decrease of the entropy generation due to the heat leakage loss is much larger than that of the increase of the entropy generation due to the friction loss, so the total optimization process is realized by decreasing the entropy generation due to heat leakage loss on the initial portion of the power stroke. (3) The optimization objective has influence on the optimal trajectory of the heat engine. The results obtained in this paper can provide some guidelines for the optimal design and operation of practical internal combustion engines.

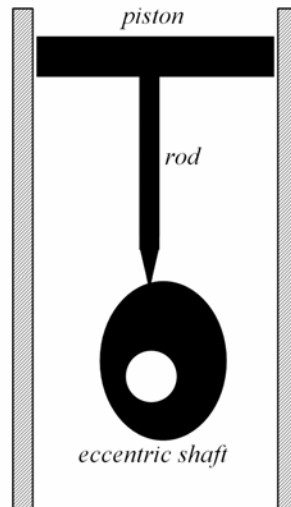


Figure 8. The mechanical transformer. An eccentric shaft of properly designed shape turns the optimal motion of the piston into a constant angular rotation

Acknowledgments

This paper is supported by The National Natural Science Foundation of P. R. China (Project No. 10905093) and the Natural Science Foundation of Naval University of Engineering (HGDYDJJ10011). The

authors wish to thank the reviewers for their careful, unbiased and constructive suggestions, which led to this revised manuscript.

Nomenclature

a	-acceleration, [m / s^2]
b	-cylinder bore, [m]
C	-constant volume heat capacity, [$kJ \cdot kg^{-1} \cdot K^{-1}$]
F	-explosion fraction, [-]
f	-friction force, [$kg \cdot m / s^2$]
G	-finite combustion rate, [m]
H	-Hamiltonian, [-]
h	-heating function, [kJ]
k	-heat transfer coefficient, [$W \cdot K / m^2$]
L	-stroke length, [m]
l	-connecting rod length, [m]
N	-number of moles of gas, [-]
n	-polytropic exponent, [-]
Q	-heat leakage, [J]
R	-gas constant, [$J \cdot mol^{-1} \cdot K^{-1}$]
r	-crankshaft length, [m]
S	-entropy generation, [$J \cdot K^{-1}$]
T	-temperature, [K]
t	-time, [ms]
v	-velocity, [m / s]
W	-work output, [J]
X	-displacement, [m]
<i>Greek symbols</i>	
ε	-the second-law efficiency, [-]
θ	-angle of crankshaft rotating, [-]
μ	-friction coefficient, [kg / s]
τ	-cycle time, [ms]
<i>Subscripts</i>	
f	-the state of combustion end
f, t_{np}	-the effect of friction loss on nonpower strokes
f, t_p	-the effect of friction loss on power stroke
i	-the state of combustion start
max	-maximum
min	-minimum
q, t_p	-the effect of heat transfer on power stroke
t_{np}	-nonpower stroke
t_p	-power stroke
$0p$	-the state of power stroke start

References

- [1] Curzon, F. L., Ahlborn, B., Efficiency of a Carnot engine at maximum power output, *Am. J. Phys.*, 43(1975), 1, pp. 22-24
- [2] Andresen, B., *et al.*, Thermodynamics for processes in finite time, *Acc. Chem. Res.*, 17(1984), 8, pp. 266-271
- [3] Bejan A., Entropy generation minimization: The new thermodynamics of finite-size devices and finite-time processes, *J. Appl. Phys.*, 79(1996), 3, pp. 1191-1218
- [4] Berry, R. S., *et al.*, Thermodynamic Optimization of Finite Time Processes, Wiley, Chichester, 1999
- [5] Chen, L., Wu, C., Sun, F., Finite time thermodynamic optimization or entropy generation minimization of energy systems, *J. Non-Equilib. Thermodyn.*, 24(1999), 4, pp. 327-359
- [6] Sieniutycz, S., Hamilton-Jacobi-Bellman framework for optimal control in multistage energy systems, *Phys. Rep.*, 326(2000), 4, pp. 165-285
- [7] Salamon, P., *et al.*, Principles of control thermodynamics, *Energy, The Int. J.*, 26(2001), 3, pp. 307-319
- [8] Hoffman, K. H., *et al.*, Optimal process paths for endoreversible systems, *J. Non-Equilib. Thermodyn.*, 28(2003), 3, pp. 233-268
- [9] Chen, L., Sun, F., *Advances in Finite Time Thermodynamics: Analysis and Optimization*, Nova Science, New York, USA, 2004
- [10] Chen, L., *Finite Time Thermodynamics Analysis of Irreversible Progresses and Cycles* (in Chinese), High Education Press, Beijing, 2005
- [11] Sieniutycz, S., Jezowski, J., *Energy Optimization in Process Systems*, Elsevier, Oxford, UK, 2009
- [12] Feidt, M., Thermodynamics applied to reverse cycle machines, a review, *Int. J. Refrig.*, 33(2010), 7, pp. 1327-1342
- [13] Andresen, B., Current trends in finite-time thermodynamics, *Angew. Chem. Int. Edit.*, 50(2011), 12, pp. 2690-2704
- [14] Radcenco, V., Vasilescu, E. E., Feidt, R., Thermodynamic optimization of direct cycles, *Thermotehnica*, (2003), 1-2, pp. 26-31
- [15] Mozurkewich, M., Berry, R. S., Finite-time thermodynamics: Engine performance improved by optimized piston motion, *Proc. Natl. Acad. Sci. U.S.A.*, 78(1981), 4, pp. 1986-1988
- [16] Mozurkewich, M., Berry, R. S., Optimal paths for thermodynamic systems: The ideal Otto cycle, *J. Appl. Phys.*, 53(1982), 1, pp. 34-42
- [17] Hoffman, K. H., Berry, R. S., Optimal paths for thermodynamic systems: The ideal Diesel cycle, *J. Appl. Phys.*, 58(1985), 6, pp. 2125-2134
- [18] Blaudeck, P., Hoffman, K. H., Optimization of the power output for the compression and power stroke of the Diesel engine, Proc. Int. Conf. ECOS'95, Volume 2: 754, Istanbul, Turkey, 1995
- [19] Teh, K. Y., Edwards, C. F., Optimizing piston velocity profile for maximum work output from an IC engine, Proc. IMECE2006, IMECE2006-13622, 2006 ASME Int. Mech. Engng. Congress and Exposition, November 5-10, Chicago, Illinois, USA, 2006
- [20] Teh, K. Y., Miller, S. L., Edwards, C. F., Thermodynamic requirements for maximum internal

- combustion engine cycle efficiency Part 1: Optimal combustion strategy, *Int. J. Engine Res.*, 9(2008), 6, pp. 449-465
- [21] Teh, K. Y., Miller, S. L., Edwards, C. F., Thermodynamic requirements for maximum internal combustion engine cycle efficiency Part 2: Work extraction and reactant preparation strategies, *Int. J. Engine Res.*, 9(2008), 6, pp. 467-481
- [22] Teh, K. Y., Edwards, C. F., An optimal control approach to minimizing entropy generation in an adiabatic internal combustion engine, *Trans. ASME J. Dyn. Sys., Meas., Contr.*, 130(2008), 4, pp. 041008
- [23] Teh, K. Y., Edwards, C. F., An optimal control approach to minimizing entropy generation in an adiabatic IC engine with fixed compression ratio, Proc. IMECE2006, IMECE2006-13581, 2006 ASME Int. Mech. Engng. Congress and Exposition, November 5-10, Chicago, Illinois, USA, 2006
- [24] Ge, Y., Chen, L., Sun, F., Optimal paths of piston motion of irreversible Otto cycle heat engines for minimum entropy generation (in Chinese), *Sci. China: Phys., Mech., Astron.*, 40(2010), 9, pp. 1115-1129
- [25] Band, Y. B., Kafri, O., Salamon, P., Maximum work production from a heated gas in a cylinder with piston, *Chem. Phys. Lett.*, 72(1980), 1, pp. 127-130
- [26] Band, Y. B., Kafri, O., Salamon, P., Finite time thermodynamics: Optimal expansion of a heated working fluid, *J. Appl. Phys.*, 53(1982), 1, pp. 8-28
- [27] Salamon, P., Band, Y. B., Kafri, O., Maximum power from a cycling working fluid, *J. Appl. Phys.*, 53(1982), 1, pp. 197-202
- [28] Aizenbud, B. M., Band, Y. B., Power considerations in the operation of a piston fitted inside a cylinder containing a dynamically heated working fluid, *J. Appl. Phys.*, 52(1981), 6, pp. 3742-3744
- [29] Aizenbud, B. M., Band, Y. B., Kafri, O., Optimization of a model internal combustion engine, *J. Appl. Phys.*, 53(1982), 3, pp. 1277-1282
- [30] Band, Y. B., Kafri, O., Salamon, P., Optimization of a model external combustion engine, *J. Appl. Phys.*, 53(1982), 1, pp. 29-33
- [31] Burzler, J. M., Hoffman, K. H., Optimal piston paths for Diesel engines. Chapter 7 'Thermodynamics of energy conversion and transport', Sienuitycz S and De vos A, eds., Springer, New York, 2000
- [32] Burzler, J. M., Performance Optimal for Endoreversible Systems, Ph. D. Thesis, University of Chemnitz, Germany, 2002, pp. 73-88
- [33] Xia, S., Chen, L., Sun, F., Maximum power output of a class of irreversible non-regeneration heat engines with a non-uniform working fluid and linear phenomenological heat transfer law, *Sci. China Ser. G: Phys., Mech., Astron.*, 52(2009), 5, pp. 708-719
- [34] Ge, Y., Chen, L., Sun, F., The optimal path of piston motion of irreversible Otto cycle for minimum entropy generation with radiative heat transfer law, Submitted to *J. Energy Inst.*
- [35] Chen, L., Sun, F., Wu, C., Optimal expansion of a heated working fluid with phenomenological heat transfer, *Energy Convers. Manage.*, 39(1998), 3/4, pp. 149-156
- [36] Song, H., Chen, L., Sun, F., Optimization of a model external combustion engine with linear phenomenological heat transfer law, *J. Energy Inst.*, 82(2009), 3, pp. 180-183
- [37] Chen, L., *et al.*, Optimization of a model internal combustion engine with linear

- phenomenological heat transfer law, *Int. J. Ambient Energy*, 31(2010), 1, pp. 13-22
- [38] Song, H., Chen, L., Sun, F., Optimal expansion of a heated working fluid for maximum work output with generalized radiative heat transfer law, *J. Appl. Phys.*, 102(2007), 9, pp. 94901
- [39] Ma, K., Chen, L., Sun, F., Optimal expansion of a heated gas under Dulong-Petit heat transfer law (in Chinese), *J. Eng. Therm. Energy Pow.*, 24(2009), 4, pp. 447-451
- [40] Chen, L., *et al.*, Optimal expansion of a heated working fluid with convective-radiative heat transfer law, *Int. J. Ambient Energy*, 31(2010), 2, pp. 81-90
- [41] Ma, K., Optimal Configurations of Engine Piston Motions and Forced Cool-down Processes, Ph. D. Thesis, Naval University of Engineering, China, 2010
- [42] Ma, K., Chen, L., Sun, F., A new solving method for optimal expansion of a heated working fluid with generalized radiative heat transfer law (in Chinese), *Chin. J. Mech. Eng.*, 46(2010), 6, pp. 149-157
- [43] Ma, K., Chen, L., Sun, F., Optimization of a model external combustion engine for maximum work output with generalized radiative heat transfer law, *J. Energy Inst.*, in press
- [44] Chen, L., Ma, K., Sun, F., Optimal expansion of a heated working fluid for maximum work output with time-dependent heat conductance and generalized radiative heat transfer law, *J. Non-Equilib. Thermodyn.*, 36(2011), 2, pp.99-122
- [45] Taylor, C. F., The Internal Combustion Engine in Theory and Practice, Volumes 1 and 2, MA, Cambridge, 1977
- [46] Biezeno, C. B., Grammel, R., Engineering Dynamics, Blackie, London, 1955, 4, pp. 2-5
- [47] Andresen, B., Rubin, M. H., Berry, R. S., Availability for finite-time processes. General theory and a model, *J. Chem. Phys.*, 87(1983), 15, pp. 2704-2713
- [48] Shen, W., Jiang, Z., Tong, J., Engineering Thermodynamics (in Chinese), High Education Press, Beijing, 2001
- [49] Radcenco V., *et al.*, New approach to thermal power plants operation regimes maximum power versus maximum efficiency. *Int. J. Therm. Sci.*, 46(2007), 12, pp. 1259-1266
- [50] Sieniutycz S., Salamon P., Advances in Thermodynamics. Volume 4: Finite Time Thermodynamics and Thermoeconomics, Taylor & Francis, New York, 1990.

Affiliation

Lingen Chen (**corresponding author**)

The College of Naval Architecture and Power, Naval University of Engineering, Wuhan 430033, P. R. China

E-mail: lgchenna@yahoo.com, lingenchen@hotmail.com

Yanlin Ge, Fengrui Sun

The College of Naval Architecture and Power, Naval University of Engineering, Wuhan 430033, P. R. China